Acta Crystallographica Section F
Structural Biology and Crystallization Communications
ISSN 1744-3091

Crystallization and preliminary X-ray diffraction analysis of a cold-adapted catalase from *Vibrio salmonicida*

Ellen Kristin Riise,[a]‡ Marit Sjo Lorentzen,[b]‡ Ronny Helland[a] and Nils Peder Willassen[a,b]*

[a]The Norwegian Structural Biology Centre, Faculty of Science, University of Tromsø, N-9037 Tromsø, Norway, and [b]Department of Molecular Biotechnology, Institute of Medical Biology, Faculty of Medicine, University of Tromsø, N-9037 Tromsø, Norway

‡ These authors contributed equally to this work.

Correspondence e-mail: nilspw@fagmed.uit.no

Received 1 November 2005
Accepted 8 December 2005
Online 23 December 2005

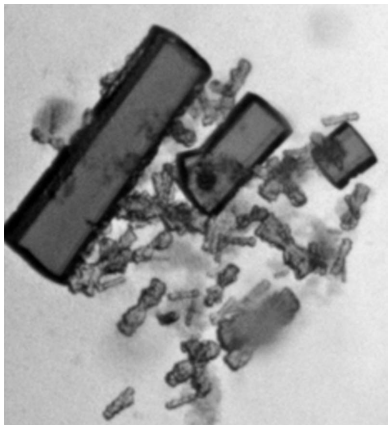

Catalase (EC 1.11.1.6) catalyses the breakdown of hydrogen peroxide to water and molecular oxygen. Recombinant *Vibrio salmonicida* catalase (VSC) possesses typical cold-adapted features, with higher catalytic efficiency, lower thermal stability and a lower temperature optimum than its mesophilic counterpart from *Proteus mirabilis*. Crystals of VSC were produced by the hanging-drop vapour-diffusion method using ammonium sulfate as precipitant. The crystals belong to the monoclinic space group $P2_1$, with unit-cell parameters $a = 98.15$, $b = 217.76$, $c = 99.28$ Å, $\beta = 110.48^\circ$. Data were collected to 1.96 Å and a molecular-replacement solution was found with eight molecules in the asymmetric unit.

1. Introduction

Catalase is present in almost all aerobic organisms and is known to protect cells against reactive oxygen species through its degradation of hydrogen peroxide to water and molecular oxygen (Deisseroth & Dounce, 1970). Three main classes of catalases have been defined: (i) the monofunctional haem-containing catalases, (ii) the bifunctional haem-containing catalases and (iii) the non-haem or manganese-containing catalases (von Ossowski *et al.*, 1993; Zamocky & Koller, 1999). The monofunctional haem-containing catalases are further subdivided into three distinct clades based on phylogenetic analysis (Klotz *et al.*, 1997). Clade I contains the plant enzymes, one algal representative and one branch of bacterial catalases. Clade II consists only of large-subunit catalases of bacterial and fungal origin, while clade III enzymes are all small-subunit catalases from bacteria, archaebacteria, fungi and other eukaryotes. Some of the catalases are able to bind NADPH and are thought to use the cofactor as protection against inactivation by its own substrate (Kirkman *et al.*, 1987; Hillar & Nicholls, 1992; Hillar *et al.*, 1994).

The crystal structures of six monofunctional haem-containing catalases of bacterial origin, those from *Escherichia coli* HPII (Bravo *et al.*, 1995), *Micrococcus lysodeikticus* (Murshudov *et al.*, 1992), *Proteus mirabilis* (Gouet *et al.*, 1995), *Pseudomonas syringae* (Carpena *et al.*, 2003), *Helicobacter pylori* (Loewen *et al.*, 2004) and *Enterococcus faecalis* (Hakansson *et al.*, 2004), have so far been determined. The structure similarity is rather high and shows that these catalases consist of four identical small or large subunits with a molecular weight in the range of 50–85 kDa, each with a prosthetic haem group deeply buried in the quaternary structure. Each subunit contains four distinct structural domains (Fita & Rossmann, 1985; Melik-Adamyan *et al.*, 1986): an amino-terminal arm (residues 1–55; *P. mirabilis* catalase numbering; Gouet *et al.*, 1995), an antiparallel eight-stranded β-barrel domain (residues 56–301), an extended structure called the wrapping domain (residues 302–416) and an α-helical domain (residues 417–484). The quaternary structure includes the interweaving of adjacent subunits that results in two tightly associated dimers per tetramer, where the four subunits are related to each other by three perpendicular dyad symmetries, the *P*, *Q* and *R* axes (Reid *et al.*, 1981) of a molecular reference frame. Small subunit-size catalases are roughly dumbbell-shaped with maximum dimensions of about 100, 80 and 100 Å along the *P*, *Q* and *R* molecular axes, respectively (Maté *et al.*, 2001).

The recombinant *Vibrio salmonicida* catalase (VSC) possesses typical cold-adapted features, with an activity curve as a function of temperature that is shifted towards low temperatures, a higher catalytic efficiency (k_{cat}/K_m) and a lower thermal stability than its mesophilic counterpart from *P. mirabilis* (PMC; unpublished results). Homology modelling (unpublished data) suggests that the VSC monomer is more flexible than that of PMC owing to a reduced number of electrostatic interactions, a less optimized core, a higher number of small residues, fewer arginines and more glycines. The PMC dimer seems to be slightly more stabilized by having a few more ion-pair interactions than the VSC dimer, whereas the VSC tetramer seems to be stabilized by an increased number of ion-pair interactions between the subunits than the PMC tetramer. Structural data at high resolution is of crucial importance in order to gain insight into the mechanisms of cold adaptation. To facilitate comparative studies between the 'warm' adapted mesophilic catalase and the cold-adapted VSC and to confirm the results from homology modelling, VSC has been crystallized with the aim of solving its three-dimensional structure by X-ray crystallography.

2. Materials and methods

2.1. Expression and purification

Catalase from *V. salmonicida* has been expressed in *E. coli* strain UM2 (*E. coli* Genetic Stock Centre, New Haven, CT, USA) using the plasmid pET-DEST42 (Gateway Technology, Invitrogen, Carlsbad, CA, USA) and the His-tagged VSC (additional amino acids = AFLYKVVINSKLEGKPIPNPLLGLDSTRTGHHHHHH) was purified to apparent homogeneity and will be published elsewhere. In brief, VSC was purified by anion-exchange chromatography (Q Sepharose), hydrophobic interaction chromatography (Phenyl Sepharose), anion-exchange chromatography (Source Q 15) and final size-exclusion chromatography (Superdex 200). The molecular weight of the His-tagged VSC monomer was determined to be 57 kDa by SDS–PAGE (data not shown). The purified protein was stored in 20 m*M* Tris–HCl pH 7.5, 250 m*M* NaCl and 5% glycerol.

2.2. Homology modelling

VSC and PMC share about 71% sequence identity, with inserts or gaps only at the ends of the C- and N-termini. A homology model of the VSC monomer generated from the structure of catalase from *P. mirabilis* (PDB code 1m85; Gouet *et al.*, 1995) was generated using *Swiss-PDBViewer* (Guex & Peitsch, 1997).

2.3. Crystallization, X-ray data collection and processing

Initial VSC crystallization conditions were obtained with the BioGenova Crystal Magic Screens I and II using the hanging-drop vapour-diffusion method. Drops consisting of 1 µl C-terminal His-tagged VSC solution (22 mg ml^{-1}) and 1 µl precipitant buffer were equilibrated against 200 µl precipitant buffer in the reservoir. Prior to X-ray data measurements the VSC crystals were cryoprotected by addition of 15%(*v*/*v*) glycerol to the precipitant buffer and flash-cooled in liquid nitrogen.

X-ray diffraction data were collected at the Swiss–Norwegian beamline (BM01A) at the European Synchrotron Radiation Facility (ESRF) using the large-scanner mode of a MAR 345 image plate. Data were recorded using 0.25° oscillation per frame, 2 min exposures and a crystal-to-detector distance of 360 mm. Data were indexed, integrated and scaled using *XDS* (Kabsch, 1993) and *SCALA* from the *CCP*4 suite (Collaborative Computational Project, Number 4, 1994). Molecular replacement was carried out using *PHASER* (McCoy *et al.*, 2005) using the homology model of VSC as a starting structure.

3. Results and discussion

Conditions for crystallization of the VSC enzyme were initially determined using the sparse-matrix approach. Several crystallization conditions were obtained from initial screenings at different temperatures. Crystals were first observed with ammonium sulfate and PEG 400 precipitant at 293–303 K. Further optimization of the conditions resulted in crystals of different shapes, sizes and quality (Fig. 1). As an attempt to improve crystal stability, 0.5 m*M* iron(II) citrate was added to the growth media in order to saturate the protoporphyrin IXs with iron. Addition of Fe^{II} to the expression media improved the crystal quality, probably owing to the presence of a more homogenic protein solution. Cocrystallization experiments with the cofactors NADPH and NADP were also set up. Crystals with or without cofactors grew in bundles, rosettes or as single crystals and appeared within two weeks. The best diffracting crystals (Fig. 1*a*) of His-tagged VSC were obtained without cofactor from 2.0 *M* ammonium sulfate, 2% PEG 400 and 100 m*M* Na HEPES pH 7.5 at 293 K with approximate dimensions of up to 0.1 × 0.4 × 0.4 mm.

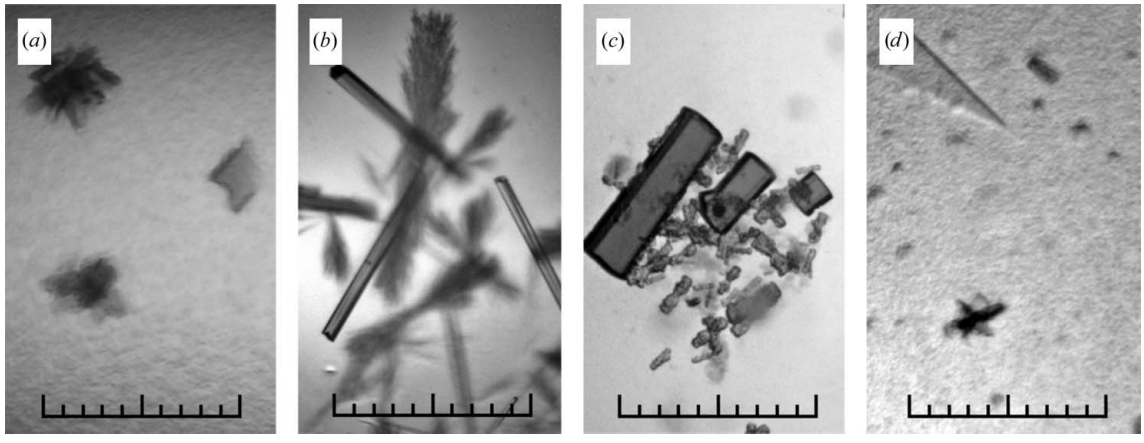

Figure 1
Crystals of *V. salmonicida* catalase grown under different conditions. (*a*) and (*d*) 100 m*M* Na HEPES pH 7.5, 2% PEG 400, 2 *M* ammonium sulfate; (*b*) 100 m*M* MES pH 5.75, 12.5% PEG 6000; (*c*) 100 m*M* HEPES pH 7.25, 17.5% PEG 6000. The scale bars are 1 mm.

Table 1
X-ray data-collection statistics for VSC.

Values in parentheses correspond to the highest resolution shells.

Beamline	BM01A
Wavelength (Å)	0.874
Space group	$P2_1$
Unit-cell parameters (Å, °)	a = 98.15, b = 217.76, c = 99.28, β = 110.48
Estimated water content (%)	50.1
Measured reflections	700080
Unique reflections	267579
Resolution range (Å)	46.8–1.96 (2.06–1.96)
Completeness (%)	95.9 (83.3)
Multiplicity (%)	2.6 (2.5)
$R_{\rm merge}$ (%)	11.1 (36.1)
Average $I/\sigma(I)$	6.0 (2.0)

The crystal without cofactor diffracted to 1.96 Å (Fig. 1*a*) and was found to belong to the monoclinic space group $P2_1$, with unit-cell parameters a = 98.15, b = 217.76, c = 99.28 Å, β = 110.48°. Data (Table 1) were 95.9% complete to 1.96 Å; $R_{\rm merge}$ was 11.1%, $I/\sigma(I)$ was 6.0 and the multiplicity was 2.6. Assuming the presence of eight molecules per asymmetric unit, the Matthews coefficient $V_{\rm M}$ is 2.50 Å^3 Da^{-1}, corresponding to a solvent content of 50.1%. The *PHASER* rotation function contained eight peaks higher than 75% of the difference between the top and the mean value. The peaks were between 6.40 and 7.80 standard deviations above the mean (Z scores), with a log-likelihood gain (LLG) between 22.02 and 33.64. The final LLG for the rotated and translated solutions was 4229.8. No significant clashes between molecules were observed.

In summary, His-tagged catalase from *V. salmonicida* crystallizes with or without cofactor in a variety of crystal forms. Most crystals were fragile and difficult to mount and in most cases diffracted poorly if diffraction could be observed at all. However, one crystal (VSC without cofactor) diffracted to 1.96 Å with reasonable scaling statistics. Further model building of VSC and refinement is in progress.

We gratefully acknowledge Jonas Jakobsen at the Department of Molecular Biotechnology, Institute of Medical Biology, University of Tromsø, Norway for technical assistance, Dr Solveig Karlsen at the Norwegian Structural Biology Centre (NorStruct), Department of Chemistry, University of Tromsø, N-9037 Tromsø, Norway for guidance and technical assistance and the Swiss–Norwegian beamlines, ESRF, Grenoble, France for providing beam time. This work was supported by The Norwegian Research Council grant 143450/140 and the National Functional Genomics Programme (FUGE) of The Research Council of Norway.

References

Bravo, J., Verdaguer, N., Tormo, J., Betzel, C., Switala, J., Loewen, P. C. & Fita, I. (1995). *Structure*, **3**, 491–502.
Carpena, X., Soriano, M., Klotz, M. G., Duckworth, H. W., Donald, L. J., Melik-Adamyan, W., Fita, I. & Loewen, P. C. (2003). *Proteins*, **50**, 423–436.
Collaborative Computational Project, Number 4 (1994). *Acta Cryst.* D**50**, 760–763.
Deisseroth, A. & Dounce, A. L. (1970). *Physiol. Rev.* **50**, 319–375.
Fita, I. & Rossmann, M. G. (1985). *J. Mol. Biol.* **185**, 21–37.
Gouet, P., Jouve, H. M. & Dideberg, O. (1995). *J. Mol. Biol.* **249**, 933–954.
Guex, N. & Peitsch, M. C. (1997). *Electrophoresis*, **18**, 2714–2723.
Hakansson, K. O., Brugna, M. & Tasse, L. (2004). *Acta Cryst.* D**60**, 1374–1380.
Hillar, A. & Nicholls, P. (1992). *FEBS Lett.* **314**, 179–182.
Hillar, A., Nicholls, P., Switala, J. & Loewen, P. C. (1994). *Biochem. J.* **300**, 531–539.
Kabsch, W. (1993). *J. Appl. Cryst.* **26**, 795–800.
Kirkman, H. N., Galiano, S. & Gaetani, G. F. (1987). *J. Biol. Chem.* **262**, 660–666.
Klotz, M. G., Klassen, G. R. & Loewen, P. C. (1997). *Mol. Biol. Evol.* **14**, 951–958.
Loewen, P. C., Carpena, X., Rovira, C., Ivancich, A., Perez-Luque, R., Haas, R., Odenbreit, S., Nicholls, P. & Fita, I. (2004). *Biochemistry*, **43**, 3089–3103.
McCoy, A. J., Grosse-Kunstleve, R. W., Storoni, L. C. & Read, R. J. (2005). *Acta Cryst.* D**61**, 458–464.
Maté, M., Murshudov, G., Bravo, J., Melik-Adamyan, V. R., Loewen, P. C. & Fita, I. (2001). *Handbook of Metalloproteins*, edited by A. Messerschmidt, R. Huber, T. Poulos & K. Wieghardt, pp. 486–502. Chichester: Wiley.
Melik-Adamyan, W. R., Barynin, V. V., Vagin, A. A., Borisov, V. V., Vainshtein, B. K., Fita, I., Murthy, M. R. & Rossmann, M. G. (1986). *J. Mol. Biol.* **188**, 63–72.
Murshudov, G. N., Melik-Adamyan, W. R., Grebenko, A. I., Barynin, V. V., Vagin, A. A., Vainshtein, B. K., Dauter, Z. & Wilson, K. S. (1992). *FEBS Lett.* **312**, 127–131.
Ossowski, I. von, Hausner, G. & Loewen, P. C. (1993). *J. Mol. Evol.* **37**, 71–76.
Reid, T. J. III, Murthy, M. R., Sicignano, A., Tanaka, N., Musick, W. D. & Rossmann, M. G. (1981). *Proc. Natl Acad. Sci. USA*, **78**, 4767–4771.
Zamocky, M. & Koller, F. (1999). *Prog. Biophys. Mol. Biol.* **72**, 19–66.